

# Usage of Industrial Computed Tomography for Evaluation of Custom-Made Implants

**Radovan Hudák, Jozef Živčák, Teodor Tóth, Jaroslav Majerník and Martin Lisý**

**Abstract** Development of additive technologies and biocompatible materials facilitated their use in the custom-made implants manufacture. Verification of custom-made implants manufactured using the additive manufacturing technologies is the key task to be fulfilled prior to the clinical application of an implant. It consists of parameters verification within individual steps, from a software design, through manufacturing, surface finishing, up to finalization of a medical product. The article presents possible uses of a 3D printing and the computed tomography (Metrotom 1500, Carl Zeiss, Germany) for the verification of selected parameters of customized implants manufactured using the Direct Metal Laser Sintering (DMLS) technology with the EOSINT M280 equipment (EOS GmbH, Germany) from the biocompatible titanium alloy Ti-6Al-4V (Grade 5). The article describes the possibilities of the computed tomography use in the verification of implant shapes and external dimensions, as well as internal structure. The internal structure means the implant porosity assessment.

---

R. Hudák (✉) · J. Živčák · T. Tóth

Faculty of Mechanical Engineering, Department of Biomedical Engineering and Measurement,  
Technical University of Košice, Letná 9, 042 00 Košice, Slovakia  
e-mail: radovan.hudak@tuke.sk

J. Živčák

e-mail: jozef.zivcak@tuke.sk

T. Tóth

e-mail: teodor.toth@tuke.sk

J. Majerník

Faculty of Medicine, Department of Medical Informatics, University in Košice, Trieda SNP 1, 040  
11 Košice, Slovakia  
e-mail: jaroslav.majernik@upjs.sk

M. Lisý

CEIT Biomedical Engineering, Tolstého 3/6, 040 01 Košice, Slovakia  
e-mail: martin.lisy@ceit-ke.sk

© Springer International Publishing Switzerland 2016

R. Bris et al. (eds.), *Applications of Computational Intelligence*  
in *Biomedical Technology*, Studies in Computational Intelligence 606,  
DOI 10.1007/978-3-319-19147-8\_2

# 1 Introduction

The development of modern imaging methods, computer-aided processing of three-dimensional (3D) data (CAD/CAM), and new manufacturing technologies (3D printing or additive manufacturing—AM) facilitated the massive growth in the production of implants and replacements for human body parts which copy anatomical structures relatively accurately [1].

Diagnostic methods most frequently used for the collection of medical data serving for the custom-made implants modelling include the computed tomography (CT) and the magnetic resonance imaging (MRI). Quality of the resulting model depends on the accuracy of diagnostic equipment and the data resolution. Reduction of the scan spacing (slice index) using the CT enables production of more slices along the diagnosed section, which increases the resolution of the obtained data. The longer the scanning period, the higher the resolution of the image; on the other hand, however, it is necessary to consider a patients exposure to the radiation, cost-depending scanning time, as well as a patients comfort [1].

An important part of the custom-made implant designing and manufacture process is the process of design evaluation (Fig. 1) consisting of the verification and validation processes. The article describes possible uses of modern technologies, such as the computed tomography, for the purpose of verification of the processes and validation of custom-made implants manufactured using the DMLS additive technology with the EOSINT M280 equipment (EOS GmbH, Germany). The case study will be presented using a custom-made cranial implant [2].

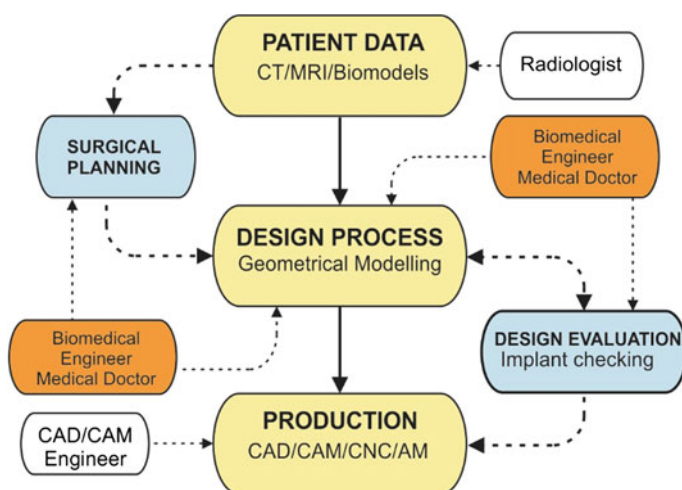


**Fig. 1** Flowchart of design and manufacturing of custom medical implant [2]

## 2 Design and Manufacturing of Custom Made Implant

Custom-made cranial implant was manufactured using the DMLS technology, from the Ti-6Al-4V titanium alloy (Grade 5). The manufacture as such was preceded by the collection of clinical CT data of a particular patient in the DICOM format which were used to create a point cloud and subsequently a CAD model [1].

Successful implant manufacture requires the elaboration of an optimal methodology of procedures and operations so that they are reproducible for the highest possible number of specific cases. This methodology includes the proposals of individual solutions, whereas the entire sequence is customised to meet the requirements imposed with regard to the final product. The comprehensive methodology proposal should take into consideration that this issue is not purely within the responsibility of a technician; it depends, above all, on the cooperation between the technician and a physician/surgeon [1].

The overall process of the custom-made implant manufacture consists of the following steps:

1. generation of a damaged section 3D model—using the CT, MRI,
2. computer-assisted implant design,
3. implant design verification,
4. implant manufacture using appropriate technology,
5. manufactured implant verification.

Computed tomography enters the designing and manufacture process as the technology facilitating the generation of input data (DICOM data) which are used as the basis for the implant designing and subsequently at continuous and final inspections of the implant [1].

In the initial modelling stage, following the collection of a patients DICOM data, the input data in the format are imported and converted into the working environment of the Mimics software (Materialise, Belgium). Prior to work with CT images in the format, it is necessary to determine proper orientation of the given images with regard to the human body planes. Afterwards, soft tissues are removed and a skull model is created (Fig. 2) [1].

Figure 3 shows a referential 3D model of a particular patients skull with a detailed image of the skull defect.

Subsequently, the cranial implant is created by gradual software-aided removing or remodeling of the 3D referential model, as specified by a doctors requirements and on the basis of a patients needs [1].

Cranial implant creation uses the so-called vertical skeletal planes that serve as the basis for creating a mirror image of the healthy skull section at the defect locations, or of a missing section.

The cranial implant design visualization based on vertical and horizontal skeletal planes with regard to the defect margins is presented in Fig. 4 [1].

The following step consisted of suggesting the positioning of the fixation mechanism, considering the sutures of the separated skull section to the skull (Fig. 5) [1].

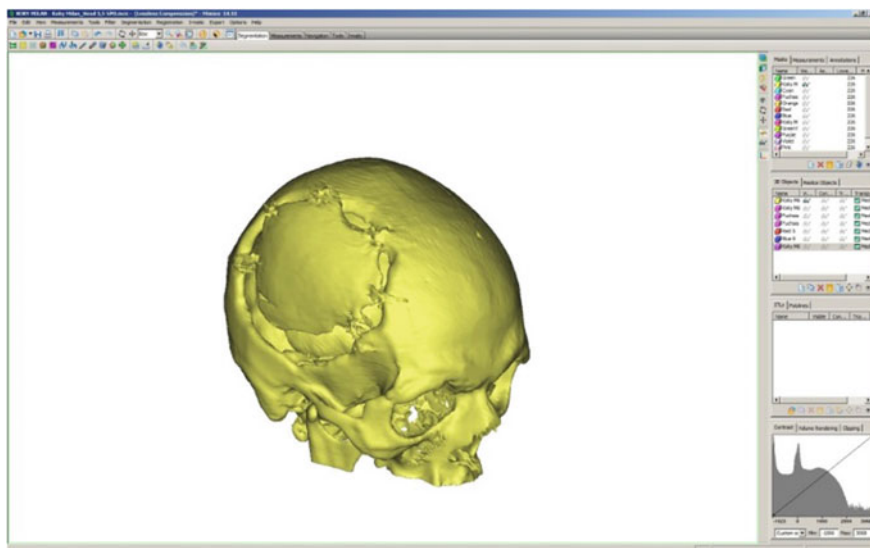
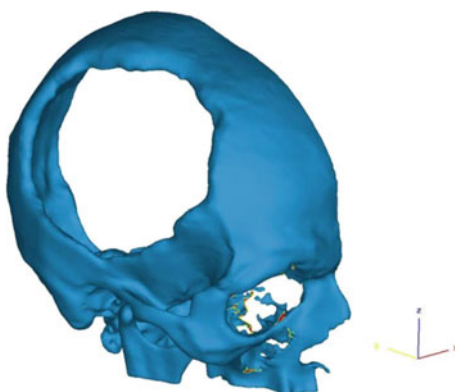


**Fig. 2** Skull model after soft tissue removal [1]

**Fig. 3** Referential CAD skull [1]



On the above mentioned fixation mechanisms, the lengths of screws protruding into both cortical bone components were defined in accurately determined positions with regard to the skull [1].

The CAD model finalisation and subsequent CAM modelling were followed by the custom-made cranial implant manufacturing using the DMLS technology [1] (Fig. 6).

**Fig. 4** Vertical and horizontal skeletal planes for implant modeling [1]

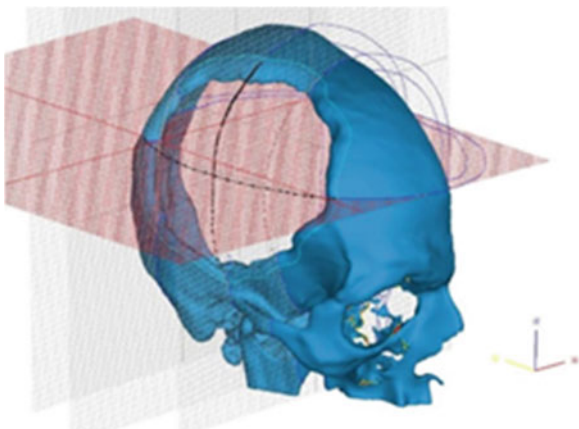


**Fig. 5** Suggested fixation mechanisms [1]

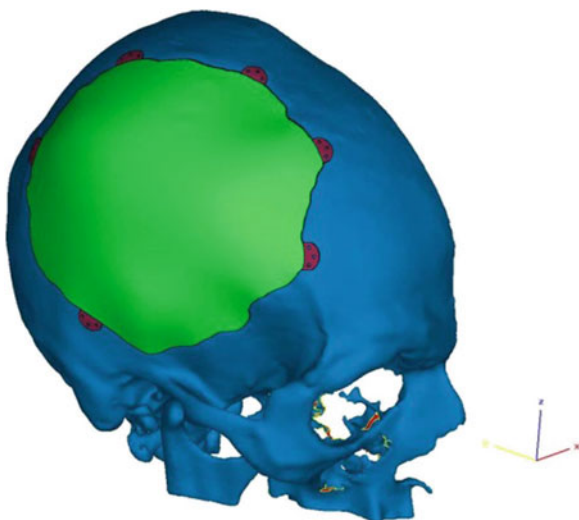
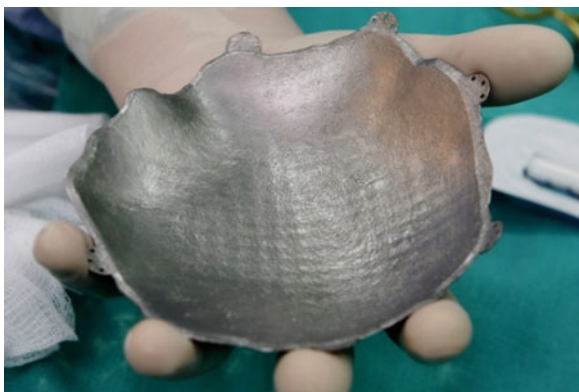


**Fig. 6** Cranial implant made of Ti-6Al-4V titanium alloy (Grade 5) [1]



### 3 Verification of the Custom—Made Cranial Implant

Unlike conventional engineering applications where majority of objects or their parts can be described using elementary 2D and 3D elements (plane, circle, roller, ...), individual implants are mostly formed of curves. Therefore, the preparation of any drawings as well as the verification of the manufactured implant by conventional measuring technologies (CMM, conventional gauges, ...) is difficult to perform. Currently, the verification of a manufactured implant can be carried out using 3D scanners and the industrial computed tomography. The use of 3D scanners is appropriate for the shape inspection, for example the shape of an implants outer surface. In case of the comprehensive inspection of the entire implant, it is appropriate to use the computed tomography that provides the data regarding the surface, as well as the content, and is less time-consuming [2, 3].

Computed tomography can be used in the three following areas:

- shape deviations inspection,
- dimensional analysis,
- thickness measurement,
- defectoscopy.

Some autors use computed tomography for evaluation of porosity in a laser sintered artifacts or implants.

Lonard et al. in study “Assessment by X-ray CT of the effects of geometry and build direction on defects in titanium ALM parts” demonstrated that X-ray computed tomography is a powerful tool for fully characterizing, in 3D, the typical defects seen in titanium ALM components. Not only can the whole specimen be examined, but the exact size, shape, maximum dimension and location of the pores can be obtained whilst it is impossible from 2D metallographic sections [4].

Slotwinski and Garboczi in “Porosity of Additive Manufacturing Parts for Process Monitoring” describe the usage of ultrasonic porosity sensor for 0,2 % change in porosity for CoCr alloy and compare it with CT [5–7].

Girardin et al. in “Characterization of Porosity in a Laser Sintered MMCp Using X-Ray Synchrotron Phase Contrast Microtomography” use for characterization of porosity in a laser sintered metal matrix composite x-ray synchrotron [8].

For shape validation only the autors use various devices like coordinate measuring machines and 3D scanners. The CMM machines measure only in few defined points and we dont obtain the whole geometry of measured object. With 3D scanners we obtain the whole surface geometry but with worster accuracy. The accuracy of scanners is given in tenths of a millimeter and the accuracy of CT is in microns.

For deviation analysis Drstvensek et al. in “Applications of Rapid Prototyping in Cranio-Maxilofacial Surgery Procedures” use for cranio-maxilofacial implat shape validation the GOM ATOS II optical scanner [9].

Salmi use in “Medical applications of additive manufacturing in surgery and dental care” Carl Zeiss C700 coordinate measuring machine for validation of plastic 3D model and the occlusal splints are verify by 3D scanners [10].

Podshivalov et al. in “Design, Analysis and Additive Manufacturing of Porous Structures for Biocompatible Micro-Scale Scaffolds” use microCT for verification of micro-scale bone scaffold printed by additive manufacturing [11].

Bauza et al. in “Study of accuracy of parts produced using additive manufacturing” use tomograph Zeiss Metrotom 1500 and coordinate measuring machine Zeiss Contura G2 for verification of two artifacts built from stainless steel on an EOS M270 machine [12].

Matilainen in his work “Benchmarking of laser additive manufacturing process—bachelor thesis” describe the specimens created for verification of different additive manufacturing processes. For verification of LAM machine he design own artifact from EOS PH1 material (stainless steel) and provide dimensional verification of artifact [13].

### ***3.1 Shape Deviation Inspection***

As it is often difficult to assess particular dimensions of custom-made implants, an alternative method used is the comparison of the manufactured implant and the CAD model. Unlike particular values obtained by measurements, the outcome of such comparison is the map of deviations documenting the differences between the manufactured implant and the model. The advantage is the provision of the spatial distribution of deviations, not only the data representing the selected locations. The comparison of the scanned component and the CAD model requires their alignment. They are most frequently aligned applying the “Best Fit” method which uses the least squares principle, i.e. the deviations between the scan and the model are mathematically segmented. This method is not appropriate in cases when the obtained scan and the 3D model significantly differ at some locations, as the calculation might, in an effort to minimize the deviations, shift the alignment and thus the result must not necessarily correspond to the reality.

In Fig. 7, the left part, represents the obtained scan of the cranial implant and the right part shows the comparison with the CAD model. More significant deviations are visible in the scanning non-homogeneity areas. Locations intended for the implant attachment to the skull are within the tolerances.

Figure 8, the left part, represents the comparison of the hip socket prosthesis and the CAD model. Significant deviations are caused by the noise resulting from the change of the implant cumulative thickness. Subsequently, the implant was locally treated.

#### **Fitting methods**

Figure 9 represents the comparison of two identical objects applying the “Best Fit” method. 3D imaging displays only halves of the objects for the visualization purposes. In this case, the shape deviation is zero.

In case of significantly different objects (Fig. 10, applying the “Best-Fit” method, their mutual shift (left) is clearly visible, as a result of the height change

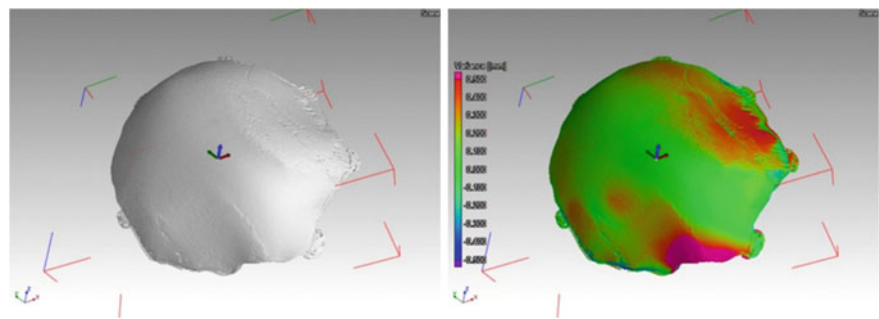


Fig. 7 Cranial implant scan (*left*), comparison (*right*)

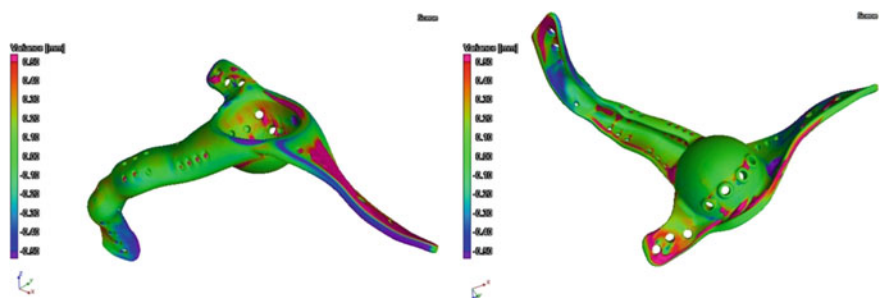


Fig. 8 Hip socket implant including a part of the Pelvis



Fig. 9 Comparison of identical objects

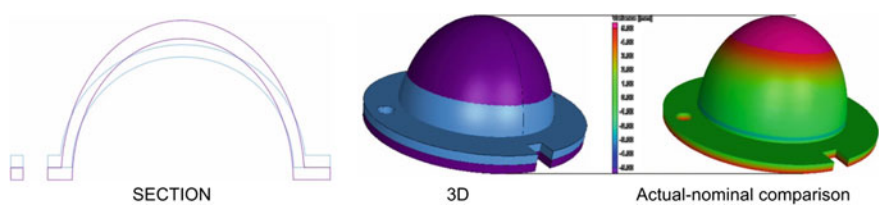
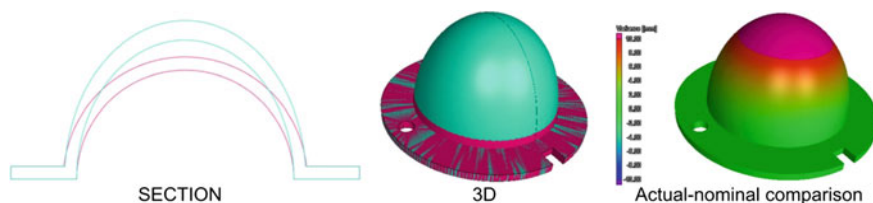
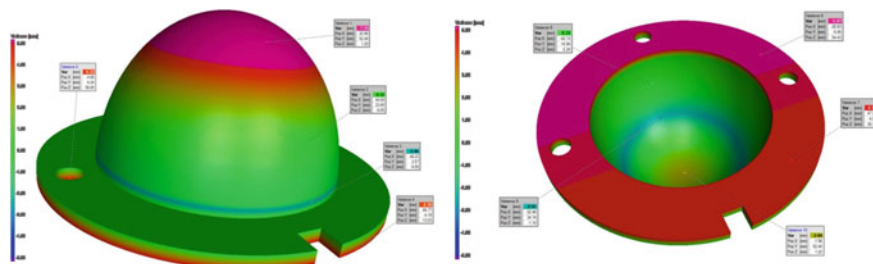


Fig. 10 “Best-fit” comparison





**Fig. 11** “Face-fit” comparison



**Fig. 12** Dimensional analysis

compensation. Consequently, this method is not suitable for the analysis. The right part of Fig. 10 represents a visible red band on the lower circular section, signaling the shift of the objects.

Figure 11 represents the comparison based on the “Face-Fit” principle, when individual objects are aligned according to the selected references. In this case, it was the alignment to the bottom plane and the groove. The left part Fig. 11. represents the cross section of the overlapping objects; the central part shows the overlap in 3D; and the right part shows the comparison of the scanned object and the 3D model, whereas the green areas fall within the tolerances, red areas are marginal, and purple areas are beyond the tolerance.

### 3.2 Dimensional Analysis

In case it is required to express numerically the values of deviations at any selected location, it is possible to use a tool enabling, after the objects are aligned and compared, the calculation and representation of a deviation at a particular location Fig. 12. If the dimensions between the components (distances) or the dimensions of individual components are required, it is appropriate to use a specialized tool, e.g. Calypso by the ZEISS Company. The dimensional analysis, however, is interesting especially in case of functional dimensions, for example the head diameter etc. in endoprosthesis.

Another option how to inspect the product is to inspect the wall thickness; for this purpose it is necessary to enter the range of the assumed thickness of the object wall

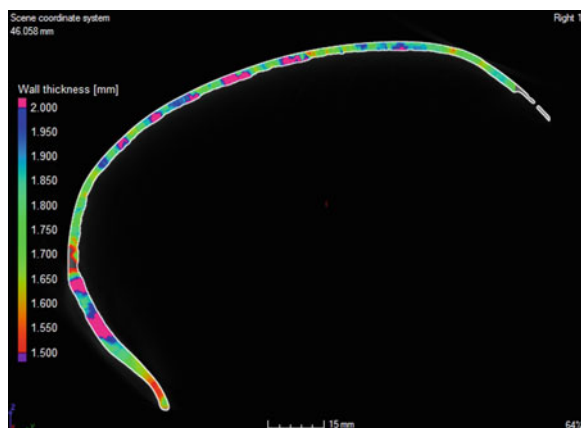
(the minimum and maximum value) and the material requirements. The thickness is evaluated as their perpendicular distance with certain permitted angle for the search thereof. In this case, the limits were set to the range of (1.5; 2.0) mm and the search angle was  $30^\circ$ .

### 3.3 Thickness Measurement

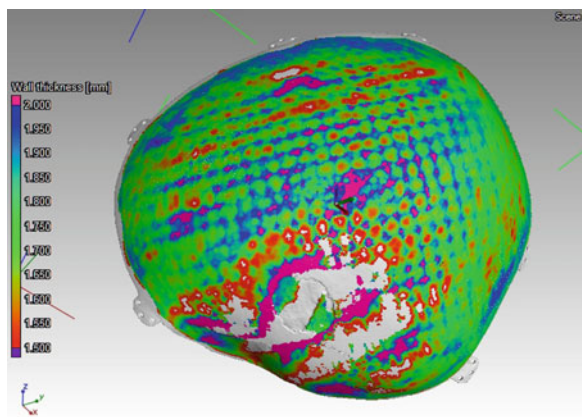
Figure 13 shows the implant cross section with the wall thickness colour coding. The cross section contains visible local changes in the wall thickness [1].

Figure 14 shows the change in the implant wall thickness along its entire surface. Clearly visible is the square mesh on the surface caused by the remains of the supporting material after it was removed from the implant inner side. The remaining material does not affect the implant functionality and thus its impact on the implant functionality is negligible [1].

**Fig. 13** Implant cross section with colour-coded wall thickness



**Fig. 14** Implant wall thickness change along the entire surface [1]



### 3.4 Defectoscopy

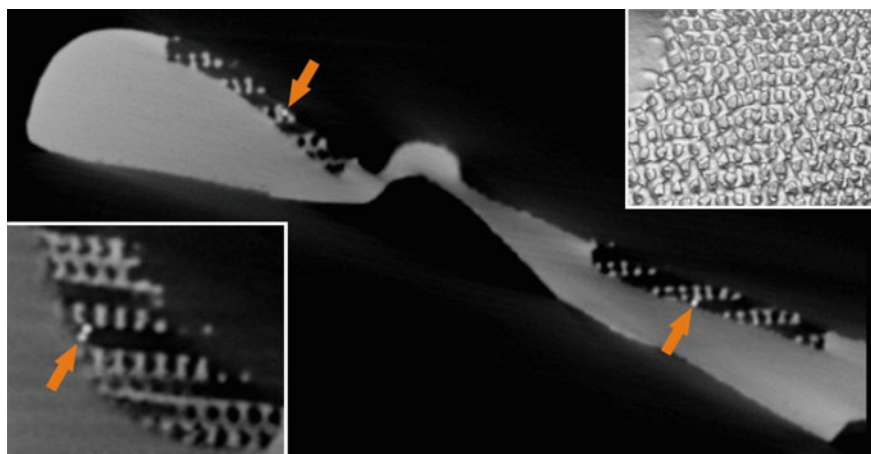
The defectoscopy means the identification of air bubbles (pores) or foreign materials (inclusion) in the basic material. Air bubbles can be formed due to imperfect manufacture, as the laser fails to fuse the building material at some locations. With regard to the fact that the implant is manufactured from the powder as the basic material, the probability of foreign material presence is minimal. Implant manufacturing is followed by the post-processing that includes also sand-blasting to reduce the surface roughness. In case of the manufacture of implants containing trabecular structures (porous structures facilitating the tissue grow through), these structures might trap the particles of the material intended for the sand-blasting. Its density is different; therefore, it can usually be identified as a significantly brighter point.

Figure 15 shows the implant cross section, while the arrows indicate the particles of the material intended for the sand-blasting. In the top right corner there is a detail of the trabecular structure, and the bottom left corner contains a detail of the inclusion from a different view.

To verify the ability to identify the defects during the manufacture process using the industrial computed tomography, an artefact containing artificial cavities was designed and subsequently manufactured.

When designing the artefact, it was necessary to consider several variables entering the manufacture process:

1. Material density—it affects the quantity of the energy required for the artefact scanning and, at the same time, it limits the minimum distance between the artefact and the X-ray tube (spot/voxel ration) and thus also the overall achieved artefact magnification on the detector.



**Fig. 15** Inclusion (sand-blasting material)

2. Artefact size—it is limited by the combination of the linear attenuation coefficient which depends on the material density and the thickness of the radiated material. Penetration of a larger sample requires more energy. Sample size is also limited by the distance from the X-ray tube and thus also the maximum artefact magnification on the detector. Proposed artefact is shown in Fig. 17.
3. Artefact orientation in the manufacture artefact orientation affects the support application and the support removal method. The orientation as such does not affect the cavities inside the artefact (Fig. 16).
4. Sizes of pores (cavities) artefact designing was carried out using the cavities of spherical shape with the diameters of 0.01 mm to 1.3 mm, evenly distributed in the artefacts volume (Fig. 17).

The artefact was manufactured in cooperation with the CEIT Biomedical Engineering s.r.o company using the Eosint M280 machine from the EOS GmbH company, and the basic material used was Ti64 titanium alloy. The artefact drawing is shown in Fig. 17.

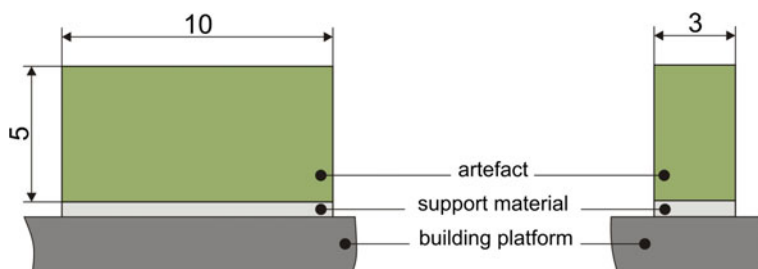


**Fig. 16** Artefact orientation in the building platform

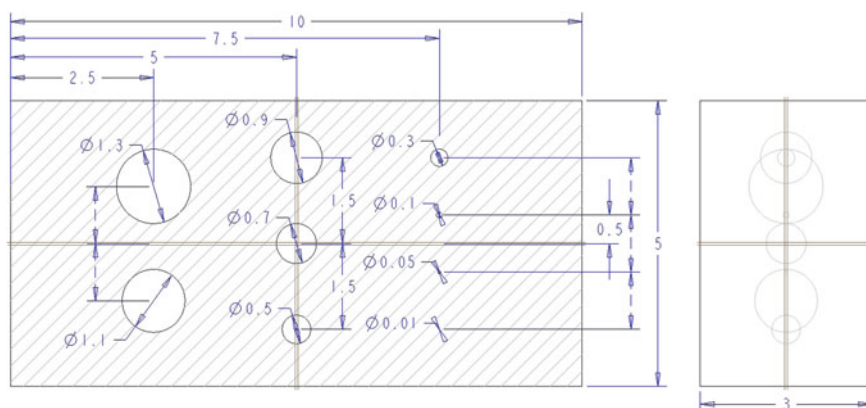


**Fig. 17** Artefact drawing

As the manufacturing is carried out layer by layer, all potential cavities are filled with unfused basic powder material. The assessment was carried out using the VGStudioMAX 2.2 software by the Volume Graphics GmbH Company.

Porosity is assessed on the basis of deviations of contrast between the material depicted in the images in grey tones and the air which is black. In case of the designed artefact, the assessment will be focused on the differences between two shades of grey, where the fused material is brighter, and thus of the density higher than the unfused material. Figure 18 shows a pore in three cross section planes and its reconstruction into 3D.

Artefact scanning was carried out using the Carl Zeiss Metrotom 1500 which was calibrated prior to the artefact scanning (detector calibration, centering, geometrical calibration, calibration of axis). Prior to the scanning, the assessed artefact was placed inside the preparation from extruded polystyrene which ensured the required stability during the scanning. The scanning consisted of two stages.

In the first stage, the artefact was scanned in the distances of 60, 200, and 600 mm from the X-ray radiation source. The scanning parameters were adjusted to the shortest possible distance between the artefact and the X-ray tube (60 mm) where a compromise between the output and the scanning distance was required. For this reason, a lower output and a longer scanning time (2,000 ms) were chosen. For other distances (200, 600 mm) the identical scanning parameters were maintained.

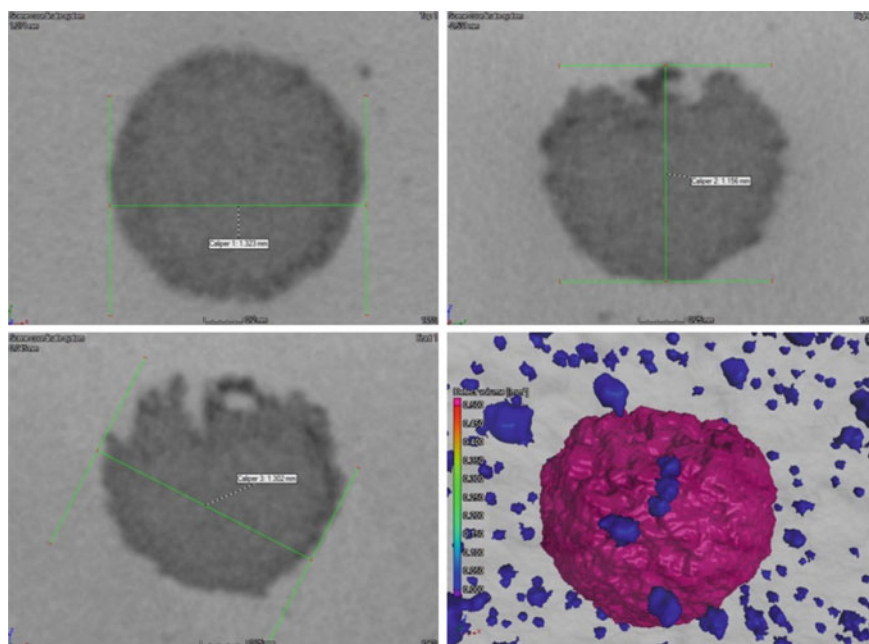


**Fig. 18** Pore representation

**Table 1** Input data table

Measurement	Distance (mm)	Voltage (kV)	Current ( $\mu$ A)	IT (ms)	Gain	Voxel ( $\mu$ m)
SN1	60	165	100	2000	16	16.39
SN2	200	165	100	2000	16	53.5
SN3	600	165	100	2000	16	159.54
SN4	200	190	280	1000	8	53.5
SN5	600	190	280	1000	8	159.54

Distance distance of object from X-Ray source

IT integration time

In the second scanning stage, the parameters were optimized for the distances of 200 and 600 mm; as a result, with the distance of 60 mm, the scanning was not possible. With regard to larger distances between the artefact and the sources, scanning parameters could be modified, whereas the applied output was increased and the scanning time was reduced down to 1,000 ms.

Scanning parameters for both stages are shown in Table 1. The data indicate that the voxel for 600 mm is approximately 10 times higher than with the distance of 60 mm, which means that while the artefact thickness of 3 mm with the distance of 60 mm consists of 183 voxels, with the distance of 600 mm it is only 18.8 voxels. This difference in number of voxels is demonstrated by the amount of obtained artefact details.

Figure 19 represents the impact of the distance on the histogram in the computer-assisted artefact reconstruction in the VGStudio SW, where the top line represents stage 1 (scanning time 2,000 ms, SN1, SN2, SN3 scans) and the bottom line represents stage 2 (scanning time 1,000 ms, SN4, SN5 scans). Due to increasing distance and thus decreasing number of voxels that form the artefact, changes occur in the histogram. With the distance of 600 mm, individual shades of grey are more significantly “depicted” in the histogram. With the distance of 600 mm, a significantly smaller powder identifying “hill” is visible than with the distances of 60 and 200 mm.

When comparing the histograms for scans with various adjustments of SN2 versus SN4 (distance of 200 mm), only a small difference is visible between the values of individual parameters (air, material, isosurface). With the distance of 600 mm and SN3 versus SN5 scans, the difference is visible also in histograms, where in the histogram for SN5, individual shades of grey are even more significantly highlighted. The histograms are shown in Fig. 19.

The results for the scanning time of 2,000 ms show that with the distance of 60 mm, the smallest assessed pore size is 0.3 mm and the smallest identifiable pore size is 0.06 mm. Smaller assessed pores cannot be identified, it means that the manufacture process is probably not able to manufacture an artificial cavity of the given size. With the scanning distance of 200 mm, the smallest identifiable pore size is 0.3 mm and with the distance of 600 mm it is 0.5 mm. Natural pores cannot be detected with the given distances.

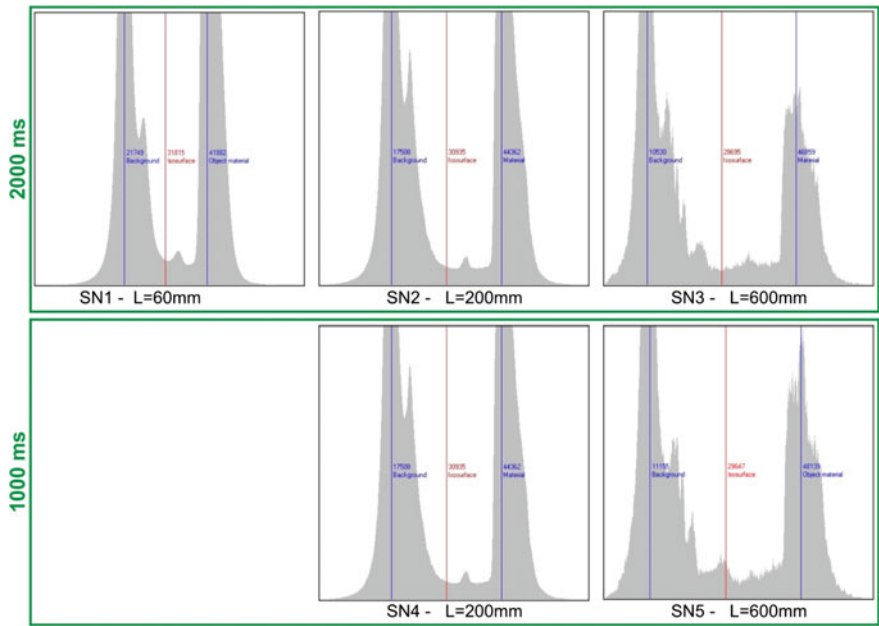


**Fig. 19** Histograms for each measurement settings (distance from X-ray source and integration time)

With the scanning time of 1,000 ms, the diameter of the smallest identifiable pore for both scanning distances is 0.5 mm. In case of 600 mm distance, however, a significant error occurs in the pore reconstruction.

Figure 20 shows the output of the porosity assessment in the distances of 60, 200, and 600 mm for individual scanning stages.

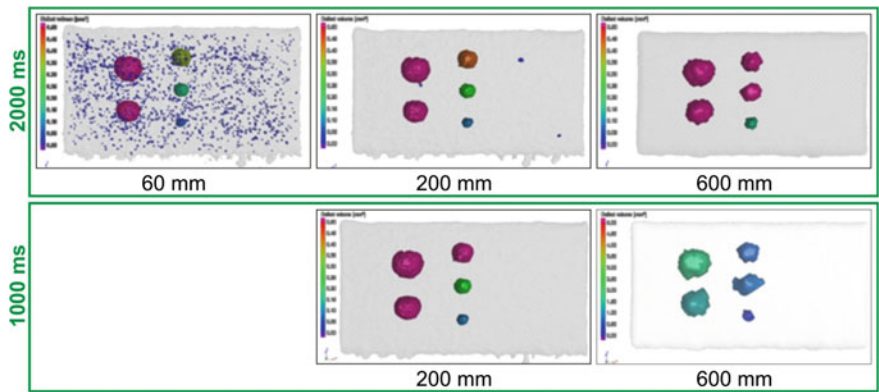


**Fig. 20** Comparison of results

## 4 Conclusion

The article suggests the possibilities of new technologies in the field of custom-made implants verification with the aim to avoid implant failure inside a patients body and protect thus not only the patient but also the manufacturer. Modern technologies, such as the computer tomography, play an important role in the implant evaluation process. They facilitate analyzing the dimensions and the shape of implants, as well as the internal material structure, with the accuracy depending on the scanning system parameters, dimensions, and shape of an implant and its position during the scanning.

Together with the simulations using CAD/CAM software and with proper application they can provide a strong tool in the process of custom-made implants verification and validation, and in the implementation in the medical ISO standards they can represent an efficient tool for implementation of additive technologies in the medical manufacture.

The results indicate that with the adjustment of appropriate input parameters for the alignment of the generated scan and the CAD model, this technology is suitable for the analyses of shape deviations, compared to the CAD model. Subsequent use of tools facilitates the generation of deviations at a random implant spot, and after the assessment requirements (tolerances) are determined, it can be assessed whether the output complies with the requirements. Dimensional analysis is not a priority in case of cranial implants, as such implants contain the minimum amount of assessable dimensions. Greater significance is assigned to the surfaces where the implant is attached to the bone, as well as the tags for the attachment to the bone. A dimension which is important in case of an acetabular cup implant is its diameter.

Computed tomography is a tool appropriate also for the identification of possible pores and inclusions in the implant. In both cases, it is necessary to consider the scanning distance, because when it increases, the equipments resolution decreases. Tiny pores in the scanning distance of 60 mm are in line with the standard specified by the equipment manufacturer. In case of control of inclusions inside the trabecular structure, a suitable choice of the scanning distance and scanning parameters is required to achieve the best possible identification. The above mentioned indicates that sometimes a particular area must be scanned several times.

**Acknowledgments** Presented paper was supported by the project Research of New Diagnostic Methods in Invasive Implantology, MSR-3625/2010-11, Stimuli for Research and Development of/( Ministry of Education, Science, Research and Sport of the Slovak Republic and project KEGA 036TUKE-4/2013, Implementation of New Technologies in Design and Fabrication of Implants in Biomedical Engineering and Related Scientific Fields and Creation and promotion of Technologies in diagnostics of components and junctions with computed tomography (ITMS:26220220038) supported by the Research & Development Operational Programme funded by the ERDF.



## References

1. Hudák, R., Živčák, J., Tóth, T., Majerník, J., Lisý, M.: Evaluation of custom-made implants using industrial computed tomography. In: Digital Technologies 2014: The 10th International Conference, 9–11 July 2014, Zilina, Piscataway, IEEE, pp. 83–87 (2014). ISBN 978-1-4799-3301-3
2. Tóth, T., Hudák, R.: Computed tomography—its development, principle and image artifacts. *Acta Mech. Slovaca. Ro.* **17**(4), 40–47 (2013). ISSN 1335-2393
3. Kruth, J.P., Bartscherb, M., Carmignatoc, S., Schmitt, R., De Chiffree, L., Weckenmann, A.: Computed tomography for dimensional metrology. *CIRP Ann. Manuf. Technol.* **60**(2), 821–842 (2011). <http://www.sciencedirect.com/science/article/pii/S0007850611002083>
4. Léonard, F., Tammas-Williams, S., Prangnell, P., Todd, I., Withers, P.: Assessment by X-ray CT of the effects of geometry and build direction on defects in titanium ALM parts. In: Conference on Industrial Computed Tomography (ICT), 19–21 Sept 2012, Wels, Austria (2012). <http://www.ndt.net/article/ctc2012/papers/91.pdf>
5. Slotwinski, J.A., Garboczi, E.J.: Porosity of additive manufacturing parts for process monitoring. In: 40th Review of Progress in Quantitative Non-Destructive Evaluation, 22–26 July 2013, Baltimore, MD (2013). [http://www.nist.gov/manuscript-publication-search.cfm?pub\\_id=914546](http://www.nist.gov/manuscript-publication-search.cfm?pub_id=914546)
6. Slotwinski, J.A.: Additive manufacturing at NIST, the science of digital manufacturing. <http://cba.mit.edu/events/13.03.scifab/Slotwinski.pdf> (2013). Accessed 7 Mar 2013
7. Brown, C., Lubell, J., Lipman, R.: Additive Manufacturing Technical Workshop Summary Report (2013)
8. Girardin, E., Renghini, C., Dyson, J., Calbucci, V., Moroncini, F., Albertini, G.: Characterization of porosity in a laser sintered MMCp using X-ray synchrotron phase contrast microtomography. *Mater. Sci. Appl.* **2**, 1322–1330 (2011)
9. Drstvensek, I., Hren, N.L., Strojnik, T., Brajlilh, T., Valentan, B., Pogacar, V., Hartner, T.Z.: Applications of rapid prototyping in cranio-maxillofacial surgery procedures. *Int. J. Biol. Biomed. Eng. Issue* <http://www.naun.org/main/NAUN/bio/bio-19.pdf>
10. Salmi M.: Medical applications of additive manufacturing in surgery and dental care. Doctoral Dissertation, Aalto university (2013). <https://aaltodoc.aalto.fi/bitstream/handle/123456789/11854/isbn9789526054964.pdf?sequence=1>
11. Podshivalov, L., Gomes, C.M., Zocca, A., Guenster, J., Bar-Yoseph, P., Fischer, A.: Design, analysis and additive manufacturing of porous structures for biocompatible micro-scale scaffolds. *Proc. CIRP* **5**, 247–252. ISSN 2212–8271. doi:10.1016/j.procir.2013.01.049
12. Bauza, M.B., Moylan, S.P., Panas, R.M., Burke, S.C., Martz, H.E., Taylor, J.S., Alexander, P., Knebel, R.H., Bhogaraju, R., O’Connell, M.T., Smokovitz, J.D.: Study of accuracy of parts produced using additive manufacturing. In: 2014 ASPE Spring Topical Meeting: Dimensional Accuracy and Surface Finish in Additive Manufacturing Berkeley, CA, United States, 13–16 April 2014. [http://www.nist.gov/manuscript-publication-search.cfm?pub\\_id=915785](http://www.nist.gov/manuscript-publication-search.cfm?pub_id=915785)
13. Matilainen, V.: Benchmarking of laser additive manufacturing process bachelor thesis. Lappeenranta University of Technology (2012). <http://www.doria.fi/bitstream/handle/10024/84863/BSc%20Thesis%20Matilainen%20fv.pdf?sequence=1>

Applications of Computational Intelligence in Biomedical  
Technology

Bris, R.; Majernik, J.; Pancerz, K.; Zaitseva, E. (Eds.)

2016, VIII, 251 p. 115 illus., 31 illus. in color., Hardcover

ISBN: 978-3-319-19146-1